

## Noncovalent Interactions between Tetrazole and an *N,N*-Diethyl-Substituted Benzamidine

Lars Peters,<sup>†</sup> Roland Fröhlich,<sup>‡</sup> Alan S. F. Boyd,<sup>§</sup> and Arno Kraft<sup>\*,†,§</sup>

*Institut für Organische Chemie und Makromolekulare Chemie II, Heinrich-Heine-Universität Düsseldorf, Universitätsstr. 1, D-40225 Düsseldorf, Germany, Organisch-Chemisches Institut der Universität, Westfälische Wilhelms-Universität Münster, Corrensstr. 40, D-48149 Münster, Germany, and Department of Chemistry, Heriot-Watt University, Edinburgh EH14 4AS, United Kingdom*

a.kraft@hw.ac.uk

Received September 1, 2000 (Revised Manuscript Received March 9, 2001)

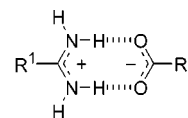
Amidines have long been known to form strong noncovalent complexes with carboxylates and phosphates. However, their interaction with tetrazoles, which are acidic heterocycles and important bioisosteric replacements for carboxylic acids in medicinal chemistry, has remained unexplored so far. The binding of a tetrazole to an *N,N*-diethyl-substituted benzamidine has been studied for the first time by X-ray crystallography, solution NMR methods, and electrospray mass spectrometry. The amidinium group of model complex **3** was found to prefer an *E,Z* configuration in the crystal. Benzamidinium and tetrazolate groups alternate along an infinite chain of hydrogen bonds and salt bridges between the amidine-NH groups and the two tetrazole-N atoms next to the ring carbon. In solution, a 1:1 complex was evident from Job's method of continuous variation, and an association constant of  $4.0 \times 10^3 \pm 1.6 \times 10^3 \text{ M}^{-1}$  (in  $\text{CDCl}_3/\text{CD}_3\text{CN}$ , 6:1) could be determined by  $^1\text{H}$  NMR dilution experiments. Tetrazolate was not only found to be a weaker ligand than carboxylates but, surprisingly, the binding mode also changed with concentration in neat  $\text{CDCl}_3$ . At low concentrations, the amidine group in complex **3** adapted an *E,E* configuration as it does in a related carboxylic acid complex **4**. With increasing concentration, the *E,Z* isomer starts to predominate. A free activation enthalpy  $\Delta G_{298}^\ddagger$  of  $64 \pm 1 \text{ kJ mol}^{-1}$  for the *E,E* to *E,Z* isomerization was determined by line shape analysis at different magnetic fields. Binding strength was further probed in a competition experiment between a bisamidine, a carboxylate, and a tetrazolate by electrospray mass spectrometry.

### Introduction

Certain acidic heterocycles are used increasingly as effective bioisosteric<sup>1</sup> replacements for carboxylic acids in medicinal chemistry. Tetrazoles<sup>2</sup> are prominent examples of this class, and four out of six angiotensin II receptor antagonists that are currently marketed for the treatment of hypertension contain a tetrazole group.<sup>3</sup> Mutagenesis studies have provided evidence that the tetrazole of a nonpeptide antagonist—like the carboxy terminus of angiotensin II—interacts with a protonated lysine and a histidine at the recognition site of the angiotensin II receptor.<sup>3a,4</sup> In this context, it is interesting

to note that the recently reported X-ray crystal structure of a tetrazole-containing inhibitor of HIV-1 integrase shows close contacts between the tetrazole's ring nitrogen atoms  $\text{N}^1$  and  $\text{N}^2$  and two lysine residues within the enzyme's catalytic domain.<sup>5</sup>

The amidine group is another important pharmacophore in modern drug design. Its complexation with carboxylates and phosphates is well established. Several X-ray crystal structures of amidinium carboxylates are known, and all conform with a binding mode in which a salt bridge is reinforced by two almost linear hydrogen bonds between carboxylate-O and amidine-NH sites.<sup>6</sup>



An *N,N*-diethyl substituted benzamidine, similar to the one chosen for the study described in this paper, has recently been introduced by Wulff et al. as the crucial binding group and base in molecularly imprinted polymers with esterase-like catalytic activity.<sup>7</sup> Compared

\* To whom correspondence should be addressed. Phone: +44-131-4518040. Fax: +44-131-4513180.

<sup>†</sup> University of Düsseldorf

<sup>‡</sup> University of Münster

<sup>§</sup> Heriot-Watt University

(1) Patani, G. A.; LaVoie, E. J. *Chem. Rev.* **1996**, *96*, 3147–3176.

(2) For general overviews of tetrazoles, see: (a) Butler, R. N. In *Comprehensive Heterocyclic Chemistry. A Review of the Literature 1982–1995*; Katritzky, A. R., Rees, C. W., Scriven, E. F. V., Storr, R. C., Eds.; Pergamon: Exeter, 1996; Vol. 4, pp 621–678. (b) Meier, H. R.; Heimgartner, H. In *Methoden der Organischen Chemie (Houben-Weyl), Heterene III/Teil 4*; Schaumann, E., Ed.; Georg-Thieme-Verlag: Stuttgart, 1994; Vol. E8d/4, pp 664–795. (c) Wittenberger, S. *J. Org. Prep. Proc. Int.* **1994**, *26*, 499–531.

(3) (a) Wexler, R. R.; Greenlee, W. J.; Irvin, J. D.; Goldberg, M. R.; Prendergast, K.; Smith, R. D.; Timmermans, P. B. M. W. M. *J. Med. Chem.* **1996**, *39*, 625–656. (b) Naka, T.; Kubo, K. *Curr. Pharm. Design* **1999**, *5*, 453–472. (c) Burnier, M.; Brunner, H. R. *Lancet* **2000**, *355*, 637–645.

(4) Noda, K.; Saad, Y.; Kinoshita, A.; Boyle, T. P.; Graham, R. M.; Husain, A.; Karnik, S. S. *J. Biol. Chem.* **1995**, *270*, 2284–2289.

(5) Goldgur, Y.; Craigie, R.; Cohen, G. H.; Fujiwara, T.; Yoshinaga, T.; Fujishita, T.; Sugimoto, H.; Endo, T.; Murai, H.; Davies, D. R. *Proc. Natl. Acad. Sci. U.S.A.* **1999**, *96*, 13040–13043.

(6) (a) Deng, Y.; Roberts, J. A.; Peng, S.-M.; Chang, C. K.; Nocera, D. G. *Angew. Chem., Int. Ed. Engl.* **1997**, *36*, 2124–2127. (b) Papoutsakis, D.; Kirby, J. P.; Jackson, J. E.; Nocera, D. G. *Chem. Eur. J.* **1999**, *5*, 1474–1480.

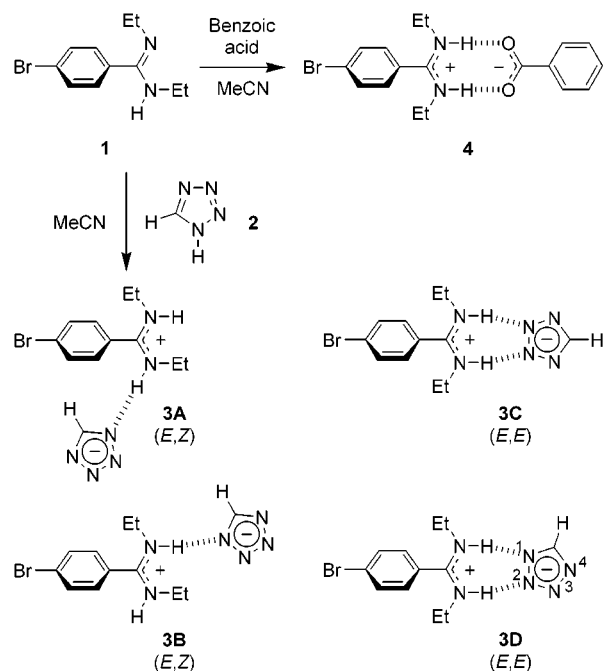
with its parent benzamidine analogue, such an *N,N*-disubstituted amidine is more soluble in nonpolar organic solvents, it has a higher stability toward hydrolysis, and aggregation is usually suppressed owing to the additional ethyl substituents. The substituted amidine derivative offers advantages in binding studies, particularly in nonpolar solvents or if weak interaction is expected.

Despite the importance of the arginine–carboxylate and amidine–carboxylate (e.g., aspartate/glutamate) interactions in protein folding and drug–receptor interactions, there has hitherto been no indication that tetrazoles show a similar affinity to arginine. At the outset of our study, it was unclear whether a tetrazole would, if pushed, bind to an amidine base in the same way as its corresponding carboxylic acid analogue. So far, little structural information is available on the complexation of a tetrazole with an amidine, a guanidine, or arginine. Whereas Arg–Gly–Asp-based tripeptides are established inhibitors of platelet aggregation, replacement of either of the two carboxylic acid groups by a tetrazole has been reported to lead to loss of activity.<sup>8</sup> Theoretical predictions by ab initio calculations have suggested that the reason behind it is a less favorable electrostatic binding between a guanidine and a tetrazolate compared to an analogous guanidinium–carboxylate complex.<sup>9,10</sup> The answer to the question how tetrazoles interact with amidines or guanidines has therefore implications for the design of new inhibitors or antagonists to natural as well as synthetic receptors. This paper describes how tetrazole (**2**) binds to an *N,N*-disubstituted benzamidine (**1**) both in the crystal and in solution. There are important differences from a related complex between **1** and benzoic acid for which a crystal structure is also presented for the first time.

## Results

**Synthesis.** Benzamidine **1** was obtained from 4-bromobenzoyl chloride in three steps following a procedure for a similar amidine derivative.<sup>11</sup> Complex **3**, a 1:1 salt,<sup>12</sup> crystallized in analytical purity upon cooling of a solution of **1** and tetrazole in warm acetonitrile (Scheme 1). Benzoic acid complex **4** and complexes of terephthalamidine **7** were prepared analogously.

**Scheme 1**



**Crystal Structures.** Slow evaporation of a methanolic solution of complex **3** gave crystals of sufficient quality for X-ray crystallography. The crystal structure is depicted in Figure 1. The C–N bond lengths of 1.31 Å (1.34 Å) for the amidinium group and 1.31 Å (1.35 Å) for the tetrazolate are characteristic of partial double bonds. Benzamidinium and tetrazolate groups alternate along an extended chain connected through almost linear (with an N5\*···H–N15 angle of 172°) and slightly bent (with an N12–H···N2 angle of 147°) hydrogen bonds. The involvement of nitrogens N2 and N5 of the tetrazole in salt bridges correlates well with theoretical calculations according to which the majority of the negative charge around the tetrazolate anion resides on the nitrogen atoms next to the ring carbon.<sup>9</sup> The short N15···N5\* and N12···N2 distances of 2.85 Å each are consistent with

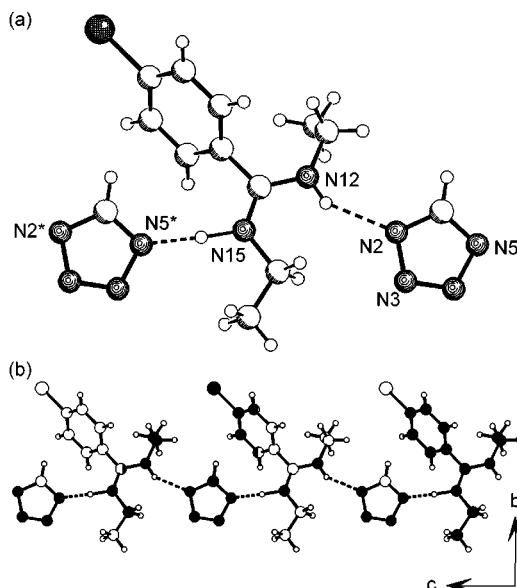


**Figure 1.** (a) Crystal structure of complex **3**. (b) Extended linear hydrogen-bonded chain of alternating molecules of **1** and tetrazole, viewed along the crystallographic *a* axis.

(7) (a) Wulff, G.; Groß, T.; Schönfeld, R. *Angew. Chem., Int. Ed. Engl.* **1997**, *36*, 1962–1964. (b) Strikovskiy, A. G.; Kasper, D.; Grün, M.; Green, B. S.; Hradil, J.; Wulff, G. *J. Am. Chem. Soc.* **2000**, *122*, 6295–6296.

(8) Two crystal structures of compounds with a guanidinium and a tetrazolate group lacked any evidence of hydrogen-bonding between the two groups: (a) Duke, J. R. *C. Chem. Commun.* **1971**, 2–3. (b) Bracuti, A. J.; Troup, J. M.; Extine, M. W. *Acta Crystallogr. C* **1986**, *42*, 505–506. For reports of crystal structures of tetrazoles hydrogen-bonded to an amine, see: (c) Chertanova, L. F.; Struchkov, Y. T.; Sopin, V. F.; Kovalenko, V. I.; Timokhov, V. N.; Fronchek, E. V. *Chem. Heterocycl. Compd.* **1995**, *31*, 655–657. (d) Parvez, M.; Unangst, P. C.; Connor, D. T.; Mullican, M. D. *Acta Crystallogr.* **1991**, *C47*, 608–611.

(9) Zablocki, J. A.; Miyano, M.; Rao, S. N.; Panzer-Knodle, S.; Nicholson, N.; Feigen, L. *J. Med. Chem.* **1992**, *35*, 4914–4917.

(10) Suvire, F.; Floridia, R.; Giannini, F.; Rodriguez, A.; Enriz, R.; Jauregui, E. *Molecules* **2000**, *5*, 583–584.

(11) (a) Wulff, G.; Schönfeld, R. *Adv. Mater.* **1998**, *10*, 957–959. (b) Schönfeld, R. Ph.D. Thesis, University of Düsseldorf, **1998**.

(12) Proton transfer was anticipated because of the two components' difference in  $pK_a$ . The  $pK_a$  value for the related protonated 4-chloro-*N,N*-dimethylbenzamidine is 11.41 (in 50% ethanol), whereas tetrazole has a  $pK_a$  of 4.89 in water: (a) Piskov, V. B.; Kasperovich, V. P.; Yakovleva, L. M. *Chem. Heterocycl. Compd.* **1976**, *12*, 917–923. (b) Lieber, E.; Patinkin, S. H.; Tao, H. H. *J. Am. Chem. Soc.* **1951**, *73*, 1792–1795.

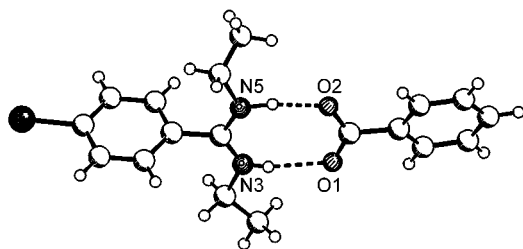


**Figure 2.** Crystal structure of complex **4**.

strong hydrogen bonds; the corresponding  $NH\cdots N$  distances are 1.65 and 2.07 Å, respectively. The only other unusually close contact stems from an electrostatic interaction between N3 of the tetrazolate anion and N15\* of a nearby cationic benzamidinium molecule at a distance of 3.38 Å.

In the crystal, the amidinium group favors an  $E,Z$  configuration with one ethyl group being nearly coplanar to the amidine whereas the  $CH_3$  residue of the other points almost perpendicularly away from the binding tetrazolate.<sup>13</sup> The torsion angle of  $66^\circ$  between amidinium group and adjacent phenyl ring is larger than for an unsubstituted amidine (ca.  $30\text{--}42^\circ$ ).<sup>6</sup> This difference clearly reflects the steric bulk of the  $N,N$ -diethyl-substituted amidine group.

A pseudo-polymorph of complex **3** suitable for X-ray crystallography could be grown from a concentrated solution in  $CDCl_3$ . One molecule of chloroform per molecule of **3** was included in the crystal, causing slight increases in torsion angles and the length of hydrogen bonds. Despite this, the binding mode was essentially the same as in Figure 1.<sup>14</sup>

The crystal structure of complex **4** is the first of a complex between a carboxylic acid and an  $N,N$ -diethyl-substituted amidine (Figure 2). The most striking feature is the  $E,E$  configuration of the amidine group, which enables the benzoate ligand to bind to the amidine through two strong H-bonds (with  $NH\cdots O$  angles of  $160^\circ$  and  $168^\circ$ ,  $NH\cdots O$  distances of 1.97 and 1.71 Å, and  $N\cdots O$  distances of 2.75 and 2.70 Å). The  $N,N$ -diethyl-substituted amidinium group has an overall zigzag conformation. The torsion angle between the NCN group and the adjacent benzene ring is, not surprisingly, even larger ( $81^\circ$ ) than in the aforementioned tetrazole complex **3** or in complexes of unsubstituted amidines with carboxylates.<sup>6b</sup>

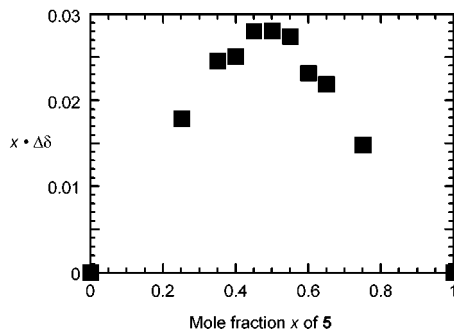
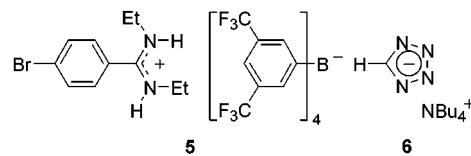
**Solution Properties of Complex 3.** A Job plot (Figure 3) supported a 1:1 stoichiometry in  $CDCl_3/CD_3CN$  (6:1).<sup>15</sup>

Figure 4 illustrates a typical NMR dilution curve of complex **3**. Nonlinear regression analysis revealed an

(13) For X-ray crystal structures of substituted amidines that emphasize a preference for the  $E_{syn}$  isomer of the amidine base and the  $E,Z$  isomer of the amidine hydrochloride, see: (a) Tinant, B.; Dupont-Fenfau, J.; Declercq, J.-P.; Podlaha, J.; Exner, O. *Collect. Czech. Chem. Commun.* **1989**, *54*, 3245–3251. (b) Trent, J. O.; Clark, G. R.; Kumar, A.; Wilson, W. D.; Boykin, D. W.; Hall, J. E.; Tidwell, R. R.; Blagburn, B. L.; Neidle, S. *J. Med. Chem.* **1996**, *39*, 4554–4562. (c) Boeré, R. T.; Klassen, V.; Wolmershäuser, G. *J. Chem. Soc., Dalton Trans.* **1998**, 4147–4154. (d) Hartmann, S.; Weckert, E.; Frahm, A. *W. Acta Crystallogr.* **1999**, *C55*, 806–808. (e) McNally, J. J.; Youngman, M. A.; Lovenberg, T. W.; Nepomuceno, D. H.; Wilson, S. J.; Dax, S. L. *Bioorg. Med. Chem. Lett.* **2000**, *10*, 213–216.

(14)  $NH\cdots N$  distances (angles): 1.84 Å ( $175^\circ$ ), 2.07 Å ( $156^\circ$ );  $N\cdots N$  distances: 2.87 and 2.85 Å. The torsion angle between NCN amidine group and the adjacent benzene ring increased to  $72^\circ$ .

(15) (a) Job, P. *Ann. Chim.* **1928**, *9*, 113–203. (b) Blanda, M. T.; Horner, J. H.; Newcomb, M. *J. Org. Chem.* **1989**, *54*, 4626–4636.



**Figure 3.** Job plot for benzamidinium salt **5** binding tetra-butylammonium tetrazolate **6**. The mole fraction  $x$  of **5** is defined as  $[5]/([5] + [6])$ . The total concentration was maintained at  $5 \times 10^{-4}$  M in  $CDCl_3/CD_3CN$  (6:1), and the change in the chemical shift  $\Delta\delta = \delta_{obsd} - \delta_0$  of the tetrazolate CH signal was determined for various compositions.

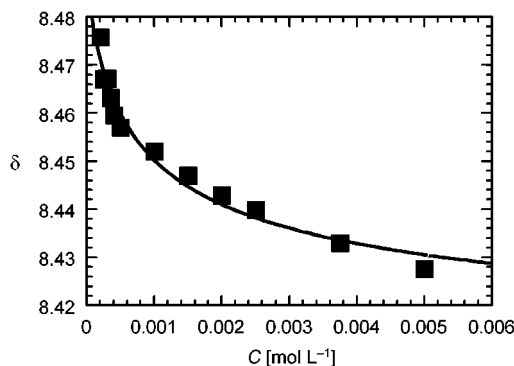


**Figure 4.** Concentration dependence of the tetrazolate CH singlet's NMR chemical shift of complex **3** in  $CDCl_3/CD_3OD$  (97:3) at  $20^\circ C$ .<sup>18</sup> The curve represents the calculated isotherm for 1:1 binding, whereas the filled squares are experimental values.

estimate for the association constant  $K_a$  of  $4.0 \times 10^3 \pm 1.6 \times 10^3 M^{-1}$  in  $CDCl_3/CD_3CN$  (6:1) and of  $1.5 \times 10^3 \pm 1.1 \times 10^3 M^{-1}$  in  $CDCl_3/CD_3OD$  (97:3) for the binding of tetrazolate to the amidinium ion.<sup>16</sup> However, anomalies occurred at higher concentration or in the absence of a polar cosolvent, and for this reason, a  $K_a$  value could not be determined in neat  $CDCl_3$  as will be discussed later. By comparison, NMR dilution studies for benzamidinium tetrazolate gave an association constant  $K_a$  of  $38 \pm 3 M^{-1}$  in  $DMSO-d_6$  for the binding of a tetrazolate to an unsubstituted benzamidinium cation.<sup>17</sup>

Two pairs of triplets and quartets are observed for the  $N$ -ethyl groups in the  $^1H$  NMR spectra of solutions of **3**

(16) The hyperbolic shape of the dilution curve was fitted to 1:1 host-guest complexation by nonlinear regression analysis: (a) Schneider, H. J.; Kramer, R.; Simova, S.; Schneider, U. *J. Am. Chem. Soc.* **1988**, *110*, 6442–6448. (b) Wilcox, C. S. In *Frontiers in Supramolecular Chemistry and Photochemistry*; Schneider, H.-J., Dürr, H., Eds.; VCH: Weinheim, 1991; pp 123–143. (c) Macomber, R. S. *J. Chem. Educ.* **1992**, *69*, 375–378.

(17) Peters, L.; Kraft, A. Unpublished results.

(18) Association constants were determined by following the tetrazolate CH singlet. Its line shape remained largely unaffected by dynamic processes of the amidine group.

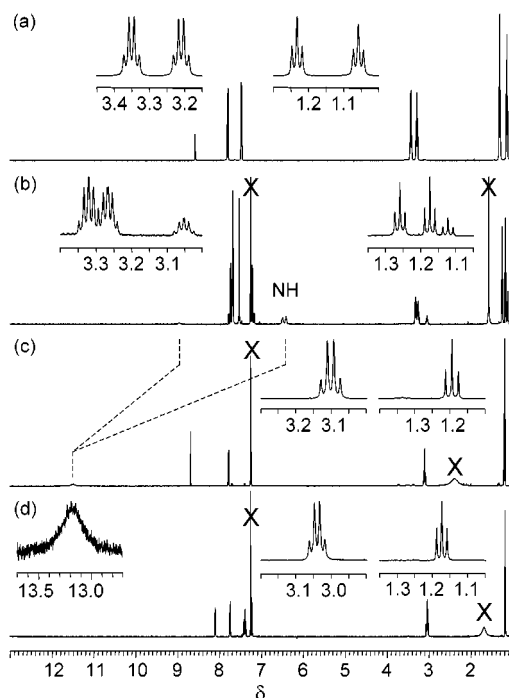


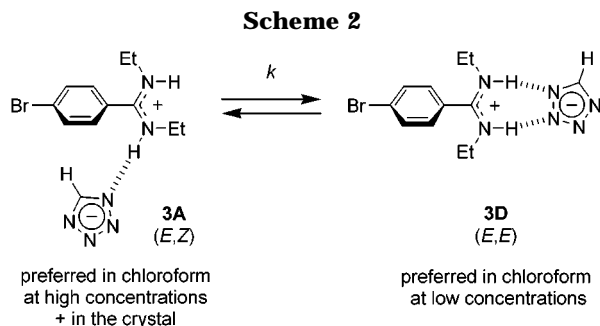
**Figure 5.**  $^1\text{H}$  NMR (500 MHz) spectra of (a) **3** in  $\text{D}_2\text{O}$ , (b) **5** in  $\text{CDCl}_3$ , (c) complex **3** in  $\text{CDCl}_3$  (0.005 M, 400 MHz), and (d) complex **4** in  $\text{CDCl}_3$ . Solvent and water signals are marked by X.

in polar solvents, such as  $\text{DMSO}-d_6$ ,  $\text{CD}_3\text{OD}$ , or  $\text{D}_2\text{O}$  (Figure 5a), indicating that the amidine exists exclusively as the *E,Z* isomer; in all these polar solvents complexation is negligible. Benzamidinium salt **5** with its non-coordinating tetrakis[3,5-bis(trifluoromethyl)phenyl]borate counteranion gives rise to more than one set of  $^1\text{H}$  NMR signals for the amidine protons in chloroform (Figure 5b). The major component is again identified as the isomer with an *E,Z* stereochemistry at the partial C–N double bonds of the amidine, whereas the minor constituent is *E,E*-configured. A *Z,Z* isomer can be excluded for steric reasons.<sup>19</sup> As Figure 5c illustrates, a solution of complex **3** in  $\text{CDCl}_3$  shows large downfield shifts of the NH signal accompanied by significant changes in isomer ratio. Although the amidine prefers an *E,Z* configuration in the crystal, the NMR data establish a predominance of the more symmetrical *E,E* isomer under conditions that favor complex formation (nonpolar solvent, coordinating counteranion). This assignment is supported by a single triplet at  $\delta_{\text{H}} = 1.19$  and a quartet at  $\delta_{\text{H}} = 3.10$  for the two *N*-ethyl groups, and it thus closely resembles the  $^1\text{H}$  NMR spectrum of benzoate complex **4** in chloroform (Figure 5d). An amidine *E,E* configuration in the benzoate complex is evident from both X-ray crystallography and solution studies.<sup>11,20</sup> We infer that complex **3** binds in chloroform, unlike in the crystal, according to binding mode **3C** or **3D** (Scheme 1) of which the latter should be more favorable since coordination of the tetrazolate through  $\text{N}^1$  and  $\text{N}^2$  results in a salt bridge that involves at least one of the more negatively charged nitrogen atoms adjacent to the ring carbon.<sup>9,21</sup>

**Amidine Isomerization.** Complexation studies, es-

(19) Hammond, G. S.; Neuman, R. C. *J. Phys. Chem.* **1963**, *67*, 1655–1659.

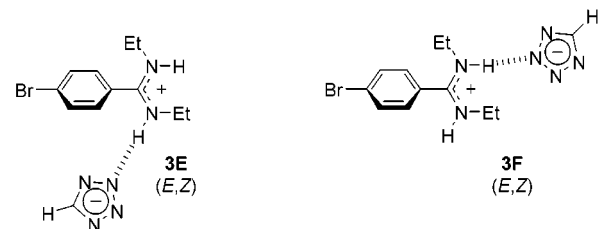
(20) Kraft, A. *J. Chem. Soc., Perkin Trans. 1* **1999**, 705–714.



pecially when carried out in neat  $\text{CDCl}_3$ , were hampered by line-broadening of the amidine's *N*-ethyl and aromatic proton NMR signals. Since ligand exchange is expected to be fast on the NMR time scale,<sup>22</sup> a dependence of the line shape on temperature and NMR frequency pointed to a dynamic process that was independent of the tetrazolate ligand, namely isomerization between the *E,E*- and *E,Z*-configured amidine (Scheme 2).<sup>11,20</sup> As mentioned before, a complex between the *E,E* isomer and tetrazole is observed in chloroform at  $5 \times 10^{-4}$  M (Figure 6a). The analysis of the NMR spectra is, however, further complicated by the fact that additional signals of the *E,Z* isomer emerged with increasing concentration (Figure 6b–d). Such a concentration-dependent change in isomer ratio has been noted for other *N,N*-disubstituted amidinium salts before.<sup>11,13d</sup> It also interfered with the determination of an association constant by a  $^1\text{H}$  NMR titration experiment in chloroform since addition of excess tetrazolate **6** similarly promoted isomerization to the *E,Z* amidine. At high concentrations, the tetrazolate singlet shifts even further upfield, which would be expected if the tetrazole proton moved into the shielding cone below the amidine's benzene ring as in isomer **3A** (or an oligomeric analogue).

We subsequently studied the temperature dependence of the  $^1\text{H}$  NMR spectra at a 0.005 M concentration of complex **3** in  $\text{CDCl}_3$ . Under these conditions, the *E,Z*-configured amidine was present as the minor component, with a ratio of 9:1 for the mixture of *E,E* and *E,Z* isomers. Whereas two of the  $\text{CH}_3$  signals overlapped, the chemical shifts of the  $\text{CH}_2$  protons were more widely spread ( $\delta_{\text{H}} = 3.10$ , 3.37, and 3.73) and could be easily extracted from

(21) In principle, tetrazolate can hydrogen-bond through either nitrogen atom  $\text{N}^1$  or  $\text{N}^2$ , and examples for both binding modes have been found in a number of crystal structures. It is as yet unclear to which extent binding through  $\text{N}^2$  may play a role in solution, but it is of little importance for the subsequent discussion on amidine isomerization. Further experiments with  $^{15}\text{N}$ -labeled tetrazoles will be necessary to clarify this point.



(22) Apart from rare cases when major conformational reorganization is necessary and dissociation constants are extremely small (i.e., in the nanomolar range), association rate constants tend to be diffusion controlled, whereas dissociation rate constants equal the quotient of the diffusion rate (around  $10^8$ – $10^9$   $\text{M}^{-1} \text{s}^{-1}$ ) and the association constant  $K_a$ : Schneider, H.-J.; Yatsimirsky, A. In *Principles and Methods in Supramolecular Chemistry*; Wiley-VCH: Weinheim, 2000; pp 259–265.

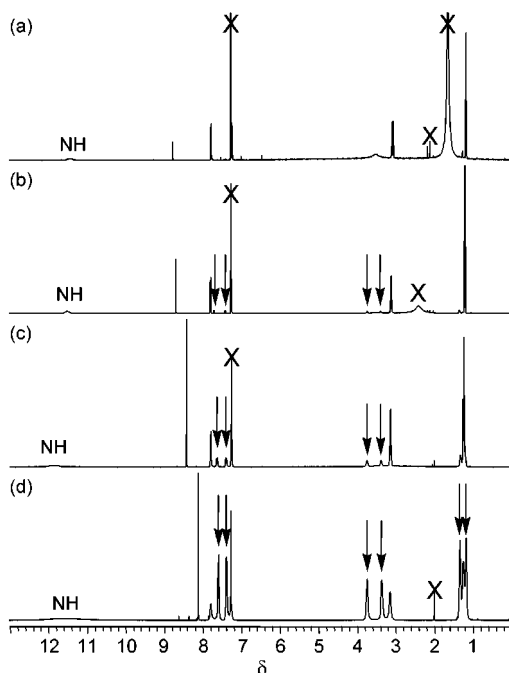


**Figure 6.**  $^1\text{H}$  NMR spectra (400 MHz, 25 °C) of **3** in  $\text{CDCl}_3$  at different concentrations: (a) 0.0005 M, (b) 0.005 M, (c) 0.02 M, and (d) 0.1 M. Solvent, water, and acetone impurity signals are marked by X. Arrows indicate signals of the (*E,Z*) isomer.

the room-temperature spectrum in the slow exchange regime (Figure 6b).<sup>23</sup> The 400 MHz  $^1\text{H}$  NMR signals of the  $\text{CH}_2$  signals coalesced upon raising the temperature to 60 °C. Line shape simulations were carried out by using the program DNMR5 to provide rates of exchange  $k$  for the isomerization between the *E,E* and *E,Z* configurations.<sup>24</sup> We deduced that both ethyl groups in the *E,Z* amidine change their environment when converting to the *E,E* isomer. Interconversion of the two ethyl groups in the *E,Z*-configured amidine was consistent with exchange cross-peaks in a two-dimensional NOESY/EXSY experiment, and simulated line shapes suggested that the rate of interconversion should be comparable to that of *E/Z* isomerization in most cases. A free activation enthalpy  $\Delta G^\ddagger$  of  $68 \pm 1 \text{ kJ mol}^{-1}$  thus derived was independent of the temperature within the errors of the  $\Delta G^\ddagger$  values.

At higher concentrations, the  $^1\text{H}$  NMR signals tended to broaden considerably even at room temperature. Since a change in temperature would invariably affect both the isomer ratio and the association constant, we conducted a further dynamic NMR experiment that allowed us to study the exchange process under conditions when these parameters remained constant. A 0.087 M sample of complex **3** in  $\text{CDCl}_3$  was hence probed at different magnetic fields (Figure 7). The high concentration of complex **3** was chosen because (i) the low-field spectrometer was not very sensitive and (ii) coalescence occurred

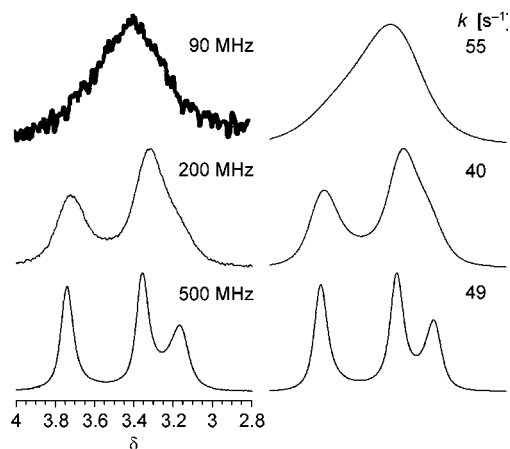


**Figure 7.** Experimental  $^1\text{H}$  NMR spectra of **3** in  $\text{CDCl}_3$  (0.087 M, 25 °C) at different NMR frequencies (left) and simulated line shapes (right).

at room temperature in the 90 MHz NMR spectrum. The chemical shifts were kept identical to those at 0.005 M, and a ratio of 1:2.7 (extracted from integrating the NMR spectrum at highest field) for the amidine's *E,E* and *E,Z* isomers was used in line shape simulations. A different magnetic field consequently alters just the frequency of the spin systems, whereas  $k$  must remain the same. Again, line shape analysis reproduced the experimental NMR spectra within a small error, thus allowing an energy barrier  $\Delta G_{298}^\ddagger$  of  $64 \pm 1 \text{ kJ mol}^{-1}$  to be calculated. The increase in line width for the amidine signals at higher concentrations was consistent with the proposed exchange process and a higher exchange rate.

**Electrospray Mass Spectra.** Electrospray ionization (ESI) mass spectrometry has become increasingly popular for the study of biological and synthetic noncovalent macromolecular complexes.<sup>25</sup> The mildness of the electrospray technique has promoted its use for screening combinatorial inhibitor libraries based on the notion that a tightly bound enzyme–inhibitor complex gives rise to a strong ion peak in the mass spectrum. Even solution binding constants have been derived from the intensities of mass ion peaks in certain cases.<sup>26</sup> A good correlation between the two has been reported for inhibitors of carbonic anhydrase as well as for a number of synthetic noncovalent complexes.<sup>27</sup>

We were able to obtain an ESI-MS of complex **3** from a solution in acetonitrile. Although the neutral complex **3** eluded detection, the dominant mass ion peaks could be identified as the singly charged (that is, protonated) base **1** +  $\text{H}^+$ ; dimer **1**<sub>2</sub> +  $\text{H}^+$ ; and a 2:1 complex **1**<sub>2</sub>·**2** +  $\text{H}^+$ . The last-mentioned cluster ion arose presumably from an association process that led to a small chain segment similar to that observed in the crystal depicted in Figure 1b.

We wondered whether it would be possible to compare the binding strength of a tetrazolate with that of a

(23) Although the signals in the aromatic region were also affected by the isomerization process, the higher order spin system proved to be too complicated for line-shape analysis.

(24) (a) Binsch, G.; Kessler, H. *Angew. Chem., Int. Ed. Engl.* **1980**, *19*, 411–428. (b) Stephenson, D. S.; Binsch, G. *J. Magn. Reson.* **1978**, *32*, 145–152. (c) Stephenson, D. S.; Binsch, G. *DNMR5: Iterative Nuclear Magnetic Resonance Program for Unsaturated Exchange-Broadened Band Shapes*, Program 365, Quantum Chemistry Program Exchange, Indiana University, Bloomington, IN.

(25) Przybylski, M.; Glocker, M. O. *Angew. Chem., Int. Ed. Engl.* **1996**, *35*, 806–826.

(26) Jørgensen, T. J. D.; Roepstorff, P.; Heck, A. J. R. *Anal. Chem.* **1998**, *70*, 4427–4432.

(27) (a) Cheng, X.; Chen, R.; Bruce, J. E.; Schwartz, B. L.; Anderson, G. A.; Hofstadler, S. A.; Gale, D. C.; Smith, R. D. *J. Am. Chem. Soc.* **1995**, *117*, 8859–8860. (b) Gao, J.; Cheng, X.; Chen, R.; Sigal, G. B.; Bruce, J. E.; Schwartz, B. L.; Hofstadler, S. A.; Anderson, G. A.; Smith, R. D.; Whitesides, G. M. *J. Med. Chem.* **1996**, *39*, 1949–1955. For examples with host–guest complexes of ammonium ions encapsulated in dimeric capsules of calixarene tetraureas, see: (c) Schalley, C. A.; Castellano, R. K.; Brody, M. S.; Rudkevich, D. M.; Siuzdak, G.; Rebek, J. *J. Am. Chem. Soc.* **1999**, *121*, 4568–4579.

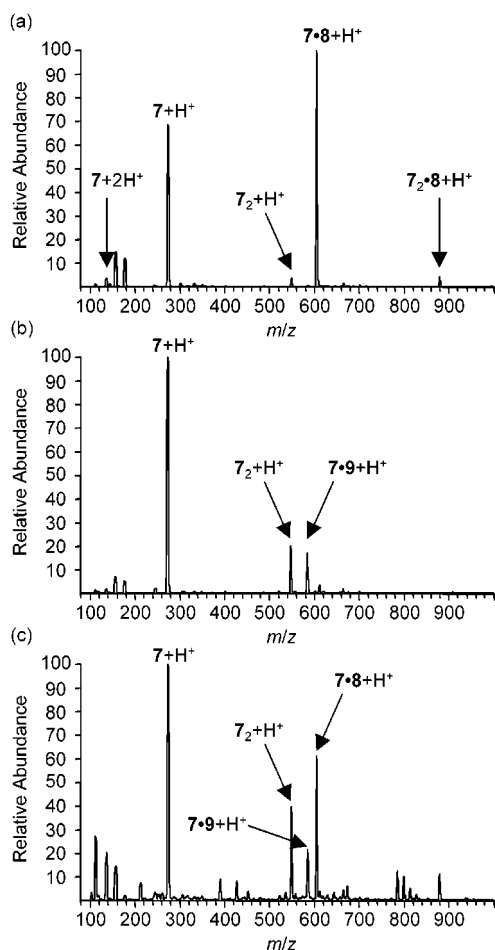
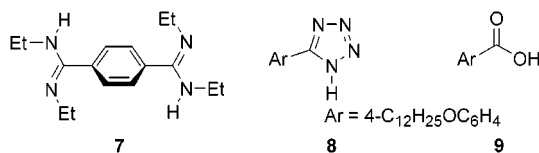


**Figure 8.** Electrospray mass spectrum of an equimolar mixture of 7–9 (in MeCN/MeOH, 80:20).

carboxylate ligand by electrospray MS since competitive solution binding studies proved to be fraught with difficulties. Detection by mass spectrometry required a 1:1 complex with an additional positively charged group that did not interfere with complexation. Our choice fell to complexes of terephthalamidine **7** with a 4-dodecyloxy-substituted phenyltetrazole **8** and an analogous benzoic acid **9**. The idea was that a protonated 1:1 complex would be left behind once a 2:1 complex lost a single benzoate or tetrazolate ligand. Figure 8a illustrates the tetrazolate–bisamidine 1:1 complex is indeed the base peak in such a case. In contrast, a benzoate–terephthalamidine 1:1 adduct gives a weaker ion peak than protonated **7** or even its dimer (Figure 8b). When an equimolar mixture of bisamidine **7**, tetrazole **8**, and carboxylic acid **9** was analyzed by ESI-MS (Figure 8c), the differences in the molecular mass of the base (**7**, 274 Da) and the two ligands (**8**, 330 Da; **9**, 306 Da) ensured that individual ions could be assigned without doubt. In this competition experiment, the tetrazolate–bisamidine complex gave a considerably larger peak than the corresponding benzoate–bisamidine 1:1 complex.



## Discussion

Like carboxylic acids, tetrazoles are capable of forming complexes with an amidine base, such as **1**. The crystal structure of our model 1:1 complex **3** reveals that the protonated amidine prefers an *E,Z* configuration in the solid state, no matter whether crystals were grown from methanol or chloroform. The high charge density on N<sup>1</sup> and N<sup>4</sup> in the tetrazolate anion, predicted by theoretical calculations,<sup>9,28</sup> explains the observed preference of these nitrogen atoms to form salt bridges with the benzamidine cations. The situation is more complicated in solution, and there it depends crucially on *solvent, ligand, temperature, and concentration*. In polar solvents or in the presence of noncoordinating counteranions the *N,N*-diethyl-substituted amidinium group exists preferably or even exclusively in the *E,Z* form, which is the sterically least hindered isomer.<sup>19</sup> However, benzoate and tetrazolate interact strongly with the amidinium group in chloroform solution. Since binding can occur through a pair of hydrogen bonds to the *E,E* isomer only, this isomer is consequently preferred.

The tetrazolate anion with its four N atoms is a flexible hydrogen-bond acceptor which adapts quite easily to different binding modes. Like a carboxylate ligand, the tetrazolate forms a complex with the *E,E*-configured amidine in chloroform at low concentration. But, as concentration increases, it binds more and more to the *E,Z* isomer instead. Tetrazolate is smaller in size and apparently less effective in forcing the amidine into an *E,E* configuration, which could be partly due to an imperfect fit compared with a carboxylate ligand. The observed change in binding mode is best explained by an oligomerization process as intercomplex hydrogen bonds are favored at higher concentrations and by a sterically less demanding *E,Z* amidine isomer. We note that an *E,Z*-configured amidine can only have a single hydrogen bond between the amidine and tetrazole (like in formulas **3A**, **3B**, or oligomeric analogues) that is reminiscent of the binding in the crystal structure. In addition, the NH signal shifts upfield again at high concentrations (Figure 6d), suggesting that the hydrogen bond weakens slightly, which conforms, too, with a change in binding mode.

Such concentration-dependent changes in isomer ratios make the determination of an association constant  $K_a$  more difficult. However, we were able to determine a  $K_a$  value of  $38 \pm 3 \text{ M}^{-1}$  for the binding of a tetrazolate to an unsubstituted benzamidine in DMSO-*d*<sub>6</sub>. The tetrazolate's binding constant thus proves to be almost 2 orders of magnitude lower than for the formation of benzamidine–benzoate complexes (with a  $K_a$  of typically about  $1550\text{--}2500 \text{ M}^{-1}$ ) in the same solvent.<sup>6</sup>

The restricted rotation around the C–N partial double bond in *N*-substituted amidines and amidinium salts has been known for a long time.<sup>13d,19,29</sup> The majority of previous studies have been carried out with highly substituted amidines since complications by tautomerization and proton exchange could thus be avoided. Rotational barriers were highly dependent on steric effects and the type of substituent on the amidine group.

(28) Arp, H. P. H.; Decken, A.; Passmore, J.; Wood, D. J. *Inorg. Chem.* **2000**, *39*, 1840–1848.

(29) (a) Harris, D. L.; Wellman, K. M. *Tetrahedron Lett.* **1968**, 5225–5228. (b) Filleux, M. L.; Naulet, N.; Dorie, J. P.; Martin, G. J.; Pornet, J.; Miginiac, L. *Tetrahedron Lett.* **1974**, 1435–1438.

An *N*-benzyl-*N,N*-dimethylbenzamidine, for example, was found to show a free activation enthalpy of around 50 kJ mol<sup>-1</sup> at the coalescence temperature, considerably less than the corresponding amidine hydrochloride (84 kJ mol<sup>-1</sup>).<sup>30</sup>

Complex **3** exhibits temperature- and field-dependent NMR spectra that are consistent with a similar dynamic process. Coalescence of the three CH<sub>2</sub> signals of the *N*-ethyl groups (and also of the CH<sub>3</sub> and aromatic proton signals, although these were not used for analysis because of considerable signal overlap) occurs at higher temperatures. The Gibbs activation barrier  $\Delta G^\ddagger$  of 68 ± 1 kJ mol<sup>-1</sup> derived from line shape analyses was comparable to that for other amidines with substituents that were more sterically demanding than methyl groups.<sup>29</sup>

Because isomer ratios and association constants are likely to be influenced by a rise in temperature, we then decided to record a number of <sup>1</sup>H NMR spectra at 25 °C, but at different magnetic fields. In this way, chemical shifts, isomer ratios, and exchange rates remain constant from one spectrum to another. However, in the case of a dynamic system, *line shapes become dependent on the spectrometer frequency* as the difference in Hz between the NMR signals varies. This is an unconventional, albeit legitimate, approach to study a dynamic process. The free activation enthalpy  $\Delta G_{298}^\ddagger$  determined for a 0.087 molar sample was thus found to be 64 ± 1 kJ mol<sup>-1</sup>. Although  $\Delta G^\ddagger$  seemed not to depend on temperature, there was a small but noticeable reduction with increasing concentration. The variable temperature and frequency NMR measurements confirmed that an *E,E* to *E,Z* isomerization was indeed responsible for the observed changes in the <sup>1</sup>H NMR line shape.

The electrospray MS results deserve further comment. They indicate that binding between the amidine and tetrazolate is stronger than formation of a benzoate–amidine complex. To explain these results, we considered that, according to <sup>1</sup>H NMR evidence, the amidine favors the *E,Z*-configuration in the polar solvent mixture (MeCN/MeOH, 80:20) used for the ESI-MS experiments. Potential ligands will therefore have to interact with this isomer under such conditions. Unlike our NMR binding studies in chloroform-rich solvents, which are dominated by hydrogen bonding and electrostatic interactions, ESI-MS measures the relative amounts of ion pairs that are not solvent-separated. Solvophobicity can consequently have a crucial effect. It is well established that tetrazolates are more lipophilic than carboxylates,<sup>1</sup> and this fact contributes to the unexpectedly stronger binding of the acidic heterocycle in MeCN/MeOH. However, an unsubstituted amidine is more likely to bind to a carboxylate ligand in the usual way through two hydrogen bonds, whereas our *N,N*-disubstituted amidine **1** describes an example when the benzoate is forced to interact in a less effective manner.

## Conclusion

The present study has demonstrated that tetrazole indeed forms a noncovalent complex with an *N,N*-disubstituted amidine, such as **1**, although association constants were found to be considerably weaker than for carboxylates. We were able to study different aspects of

binding in tetrazole–amidine complexes in the crystal, in nonpolar (chloroform), and in the presence of more competitive solvents. Although the acidic heterocycle behaves like a carboxylic acid in many respects, the mode of binding to amidine **1** surprisingly differed in the crystal and in solution. Under certain conditions tetrazolate was able to bind to an amidine through two hydrogen-bonds in a manner similar to carboxylates. It is expected that tetrazoles interact similarly with unsubstituted benzamidines and guanidines. The knowledge of possible binding modes that can be adapted by tetrazoles should be of considerable value for a better understanding of tetrazole drugs in medicinal chemistry and in synthetic enzyme mimetics.

## Experimental Section

**General Methods.** All solvents were dried and freshly distilled before use. DSC: Mettler TC 11 with TA 4000 Processor. NMR: Bruker AC200, DPX 400, DRX 500. TMS was used as chemical shift reference in the NMR measurements. The multiplicities of <sup>13</sup>C signals were determined by DEPT experiments. IR: Bruker Vector 22 FT-IR. CI-MS: Finnigan INCOS 50. ESI-MS: Thermoquest Automass benchtop LC/GC MS. Elemental analyses: Pharmazeutisches Institut der Heinrich-Heine-Universität Düsseldorf.

**4-Bromo-*N*-ethylbenzamide.** The compound was prepared by a modified literature procedure.<sup>31</sup> 4-Bromobenzoyl chloride (10.3 g, 46.7 mmol) was added portionwise over 10 min to an ice-cold aqueous solution of ethylamine (70%, 35 mL, 0.63 mol). The solution was heated to reflux, diluted with water (50 mL), and cooled to room temperature. The precipitate was collected by suction filtration, washed with water (2 × 30 mL), and dried. Yield: 9.96 g (93%), colorless solid.

**Ethyl 4-Bromo-*N*-ethylbenzimidate.** A solution of 4-bromo-*N*-ethylbenzamide (4.56 g, 20.0 mmol) and triethylxonium tetrafluoroborate (5.70 g, 30.0 mmol) in dry CH<sub>2</sub>Cl<sub>2</sub> (30 mL) was stirred for 24 h under argon at room temperature. The mixture was concentrated in a vacuum, and the residue was treated with ice-cold NaOH (3 M, 20 mL) and extracted with ether (100 mL). The organic layer was dried over Na<sub>2</sub>SO<sub>4</sub> and concentrated again. The product was distilled (Kugelrohr, 170 °C/0.02 mbar) and, because of its moisture sensitivity, used without further purification. Yield: 3.39 g (66%). <sup>1</sup>H NMR (500 MHz, CDCl<sub>3</sub>):  $\delta$  1.06 (t, *J* = 7.3 Hz, 3 H), 1.25 (t, *J* = 7.1 Hz, 3 H), 3.19 (q, *J* = 7.3 Hz, 2 H), 4.14 (q, *J* = 7.1 Hz, 2 H), 7.14, 7.47 (AA'XX', 2 × 2 H).

**4-Bromo-*N,N*-diethylbenzamidinium (1).** A solution of ethyl 4-bromo-*N*-ethylbenzimidate (3.39 g, 13.2 mmol) and ethylamine hydrochloride (2.81 g, 34.4 mmol) in dry ethanol (30 mL) was stirred for 5 days at room temperature. The mixture was concentrated in a vacuum, and the residue was suspended in ethyl acetate (100 mL) and washed with 6 N NaOH (20 mL). The organic layer was dried over Na<sub>2</sub>SO<sub>4</sub> and concentrated in a vacuum. The crude product was then purified by gradient sublimation at 110 °C/10<sup>-4</sup> mbar. Yield: 3.08 g (91%), colorless solid. Mp (DSC): 86 °C ( $\Delta H_{95}$  J g<sup>-1</sup>). <sup>1</sup>H NMR (200 MHz, CD<sub>3</sub>OD):  $\delta$  1.11 (br t, *J* ≈ 7.1 Hz, 6 H), 3.13 (br q, *J* ≈ 7.1 Hz, 4 H), 7.23, 7.60 (AA'XX', 2 × 2 H). <sup>13</sup>C NMR (50 MHz, CD<sub>3</sub>OD):  $\delta$  16.3 (broad), 130.9, 132.7 (CH, CH<sub>3</sub>), 41.3 (broad, CH<sub>2</sub>), 124.1, 136.4, 161.4 (*ipso*-C, C=N). MS (CI, NH<sub>3</sub>): *m/z* 257, 255 (M+H<sup>+</sup>). IR (KBr, cm<sup>-1</sup>):  $\nu$  3200, 3011, 2955, 2920, 1617, 1546, 1482, 1311, 1012, 826. Anal. Calcd for C<sub>11</sub>H<sub>15</sub>BrN<sub>2</sub> (255.15): C, 51.78; H, 5.93; N, 10.98. Found: C, 51.68; H, 5.99; N, 10.84. Hydrochloride **1**·HCl was obtained as a colorless solid by freeze-drying a solution of **1** in aqueous HCl. Mp (DSC): 193 °C ( $\Delta H_{83}$  J g<sup>-1</sup>). <sup>1</sup>H NMR (500 MHz, DMSO-*d*<sub>6</sub>):  $\delta$  1.08 (t, *J* = 7.1 Hz, 3 H), 1.22 (t, *J* = 6.1 Hz, 3 H), 3.12 (q, *J* = 6.1 Hz, 2 H), 3.40 (q, *J* = 7.1 Hz, 2 H), 7.55, 7.84 (AA'XX', 2 × 2 H), 9.46 (br s, 2 H). <sup>13</sup>C NMR (50 MHz,

(30) McKennis, J. S.; Smith, P. A. S. *J. Org. Chem.* **1972**, *37*, 4173–4178.

(31) Beak, P.; Musick, T. J.; Chen, C.-W. *J. Am. Chem. Soc.* **1988**, *110*, 3538–3542.

CD<sub>3</sub>OD):  $\delta$  13.2, 15.8, 131.2, 133.8 (CH, CH<sub>3</sub>), 39.4, 41.9 (CH<sub>2</sub>), 127.9, 128.7, 164.7 (*ipso*-C, C=N). IR (KBr, cm<sup>-1</sup>):  $\nu$  2982, 3100–2500 (broad), 1637 (broad), 1495, 1439, 1146, 1012, 839. Anal. Calcd for C<sub>11</sub>H<sub>16</sub>BrClN<sub>2</sub> (291.61): C, 45.31; H, 5.53; N, 9.61. Found: C, 45.11; H, 5.41; N, 9.38.

**Complex 3.** 4-Bromo-*N,N*-diethylbenzamidinium **1** (400 mg, 1.57 mmol) and **2** (110 mg, 1.57 mmol) were dissolved in hot acetonitrile (20 mL). Upon cooling to room temperature, the complex crystallized and was isolated by suction filtration. Yield: 408 mg (80%). DSC: 87 °C/*T<sub>g</sub>*/132 ( $\Delta H$  15 J g<sup>-1</sup>)/K/174 °C ( $\Delta H$  96 J g<sup>-1</sup>)/I. <sup>1</sup>H NMR (500 MHz, D<sub>2</sub>O):  $\delta$  1.14 (t, *J* = 7.3 Hz, 3 H), 1.32 (t, *J* = 7.3 Hz, 3 H), 3.29 (q, *J* = 7.3 Hz, 2 H), 3.42 (q, *J* = 7.3 Hz, 2 H), 7.47, 7.80 (AA'XX', 2 × 2 H), 8.58 (s, 1 H). <sup>13</sup>C NMR (125 MHz, CD<sub>3</sub>OD):  $\delta$  13.4, 15.9, 131.3, 134.2, 150.2 (CH, CH<sub>3</sub>), 39.5, 42.2 (CH<sub>2</sub>), 128.3, 129.1, 165.2 (*ipso*-C, C=N). IR (KBr, cm<sup>-1</sup>):  $\nu$  2978, 2792, 1637, 1495, 1439, 1147, 1011, 837. Anal. Calcd for C<sub>12</sub>H<sub>17</sub>BrN<sub>6</sub> (325.21): C, 44.32; H, 5.27; N, 25.84. Found: C, 44.26; H, 5.50; N, 25.71.

**Complex 4.** Prepared from **1** and benzoic acid. Yield: 95% (from MeCN). Mp (DSC): 159 °C ( $\Delta H$  75 J g<sup>-1</sup>). <sup>1</sup>H NMR (500 MHz, CDCl<sub>3</sub>):  $\delta$  1.18 (t, *J* = 7.3 Hz, 6 H), 3.04 (q, *J* = 7.3 Hz, 4 H), 7.22, 7.74 (AA'XX', 2 × 2 H), 7.35–7.45 (m, 3 H), 8.05–8.15 (m, 2 H), 13.2 (br s, 2 H). IR (KBr, cm<sup>-1</sup>):  $\nu$  2980, 2938, 1676, 1380, 721. Anal. Calcd for C<sub>18</sub>H<sub>21</sub>BrN<sub>2</sub>O<sub>2</sub> (377.28): C, 57.30; H, 5.61; N, 7.43. Found: C, 57.03; H, 5.76; N, 7.14.

**4-Bromo-*N,N*-diethylbenzamidinium Tetrakis[3,5-bis-(trifluoromethyl)phenyl]borate (5).** A mixture of **1**·HCl (130 mg, 0.45 mmol) and potassium tetrakis[3,5-bis(trifluoromethyl)phenyl]borate<sup>32</sup> (402 mg, 0.45 mmol) were dissolved in methanol (25 mL) and concentrated in a vacuum. The residue was then suspended in a 1:1 mixture of CHCl<sub>3</sub>/MeCN and passed through a membrane filter. The filtrate was concentrated in a vacuum, and the remaining colorless amorphous solid was dried. Yield: 480 mg (96%). <sup>1</sup>H NMR (500 MHz, CDCl<sub>3</sub>) major (*E,Z*) isomer:  $\delta$  1.17 (t, *J* = 7.2 Hz, 3 H), 1.26 (t, *J* = 7.2 Hz, 3 H), 3.27 (qd, *J* = 7.2, 5.3 Hz, 2 H), 3.32 (qd, *J* = 7.2, 6.3 Hz, 2 H), 6.42 (br s, 1 H), 6.50 (br s, 1 H), 7.22, 7.74 (AA'XX', 2 × 2 H), 7.54 (br s, 4 H), 7.69 (br s, 8 H); a set of additional signals could be assigned to the minor (*E,E*) isomer:  $\delta$  1.12 (t, *J* = 7.3 Hz, 6 H), 3.05 (qd, *J* = 7.3, 6.3 Hz, 4 H), 7.17, 7.78 (AA'XX', 2 × 2 H), 8.96 (br s, 2 H). IR (KBr, cm<sup>-1</sup>)  $\nu$  2997, 1639, 1356, 1279, 1121, 887, 838, 712, 682, 671. Anal. Calcd for C<sub>43</sub>H<sub>29</sub>BBrF<sub>24</sub>N<sub>2</sub> (1119.37): C, 46.14; H, 2.52; N, 2.50. Found: C, 46.12; H, 2.51; N, 2.63.

**Tetrabutylammonium Tetrazolate (6).** A solution of tetrazole (2.10 g, 30.0 mmol), aqueous tetrabutylammonium hydroxide (40%, 19.8 mL, 30.0 mmol), and NaOH (6 M, 10 mL) was extracted with CHCl<sub>3</sub> (200 mL). The organic extract was then concentrated in a vacuum to afford **6** (9.00 g, 97%) as a colorless amorphous solid that, owing to its hygroscopicity, was stored under argon. <sup>1</sup>H NMR (500 MHz, CDCl<sub>3</sub>):  $\delta$  0.97 (t, *J* = 7.6 Hz, 12 H), 1.38 (tq, *J* = 6.9, 7.6 Hz, 8 H), 1.49–1.56 (m, 8 H), 3.10 (m, 8 H), 8.35 (s, 1 H). <sup>13</sup>C NMR (125 MHz, CDCl<sub>3</sub>):  $\delta$  13.6, 19.7, 23.9, 58.6, 149.8. IR (KBr, cm<sup>-1</sup>):  $\nu$  2962, 2875, 1487, 1470, 1421, 1383, 1140, 1109, 882, 748. Anal. Calcd for C<sub>17</sub>H<sub>37</sub>N<sub>5</sub>·0.5 H<sub>2</sub>O: C, 63.71; H, 11.95; N, 21.84. Found: C, 63.73; H, 11.66; N, 21.76.

**Complex between *N,N,N',N'*-Tetraethylterephthalamidine (7)<sup>33</sup> and 5-(*p*-Dodecyloxyphenyl)tetrazole (8).<sup>34</sup>** Yield: 83% (MeCN/MeOH). DSC: *K*<sub>1</sub>/86 °C ( $\Delta H$  35 J g<sup>-1</sup>)/*K*<sub>2</sub>/133 °C ( $\Delta H$  14 J/g)/I. <sup>1</sup>H NMR (500 MHz, CDCl<sub>3</sub>/CD<sub>3</sub>OD, 6:1):  $\delta$  0.89 (t, *J* = 6.8 Hz, 6 H), 1.10 (br s, 12 H), 1.20–1.40 (m, 24

H), 1.40–1.50 (m, 4 H), 1.70–1.90 (m, 4 H), 3.12 (br s, 4 H), 3.48 (br s, 4 H), 4.00 (t, *J* = 6.8 Hz, 4 H), 6.96, 7.93 (AA'XX', 2 × 4 H), 7.48 (s, 4 H). IR (KBr, cm<sup>-1</sup>):  $\nu$  2923, 2851, 1638, 1536, 1443, 1249, 838. Anal. Calcd for C<sub>50</sub>H<sub>78</sub>N<sub>12</sub>O<sub>2</sub>·H<sub>2</sub>O: C, 66.93; H, 8.99; N, 18.73. Found: C, 66.86; H, 9.19; N, 18.42.

**Complex between 7<sup>33</sup> and *p*-Dodecyloxybenzoic Acid (9).<sup>35</sup>** Yield: 70% (MeCN). Mp (DSC): 136 °C ( $\Delta H$  130 J g<sup>-1</sup>). <sup>1</sup>H NMR (500 MHz, CDCl<sub>3</sub>/CD<sub>3</sub>OD, 6:1):  $\delta$  0.80 (t, *J* = 6.7 Hz, 6 H), 1.00–1.32 (m, 44 H), 1.35–1.45 (m, 4 H), 1.65–1.75 (m, 4 H), 3.92 (t, *J* = 6.5 Hz, 4 H), 6.80, 7.86 (AA'XX', 2 × 4 H), 7.54 (br s, 4 H). IR (KBr, cm<sup>-1</sup>):  $\nu$  2922, 2852, 1681, 1645, 1606, 1255. Anal. Calcd for C<sub>54</sub>H<sub>86</sub>N<sub>4</sub>O<sub>6</sub>·3 H<sub>2</sub>O: C, 68.90; H, 9.85; N, 5.84. Found: C, 69.10; H, 9.64; N, 5.84.

**Determination of Association Constants.** NMR dilution experiments were carried out with complex **3**, which contained exactly equimolar amounts of amidinium and tetrazolate ions. Nonlinear regression analysis [with Kaleidagraph version 3.5 (Synergy Software)] was used to fit the concentration *C* of complex **3** and the experimental <sup>1</sup>H NMR chemical shifts  $\delta$  of the tetrazole CH singlet in the unbound ( $\delta_0$ ) and the complexed form ( $\delta_c$ ) to the equation<sup>16</sup>

$$\delta = \delta_0 - \frac{\delta_0 - \delta_c}{2K_a C} \cdot [2K_a C + 1 - \sqrt{4K_a C + 1}]$$

**Single-crystal X-ray diffraction analysis of 3:** formula C<sub>12</sub>H<sub>17</sub>BrN<sub>6</sub>, *M* = 325.23, colorless needle 0.35 × 0.10 × 0.05 mm, *a* = 11.225(5) Å, *b* = 14.226(5) Å, *c* = 9.112(2) Å, *V* = 1455.1(9) Å<sup>3</sup>,  $\rho_{\text{calcd}}$  = 1.485 g cm<sup>-3</sup>,  $\mu$  = 38.29 cm<sup>-1</sup>, empirical absorption correction via  $\psi$  scan data (0.348 ≤ *T* ≤ 0.832), *Z* = 4, orthorhombic, space group *Pna*2<sub>1</sub> (No. 33),  $\lambda$  = 1.54178 Å, *T* = 223 K,  $\omega/2\theta$  scans, 1566 reflections collected (+*h*, +*k*, +*l*), [(sin  $\theta$ )/ $\lambda$ ] = 0.62 Å<sup>-1</sup>, 1566 independent and 1351 observed reflections [*I* ≥ 2 $\sigma$ (*I*)], 183 refined parameters, *R* = 0.038, *wR*<sup>2</sup> = 0.106, maximum residual electron density 0.43 (−0.78) e Å<sup>-3</sup>, Flack parameter −0.01(4). Hydrogens were found at the nitrogen atoms from difference Fourier calculations, others were calculated and refined as riding atoms.

**Single-crystal X-ray diffraction analysis of 4:** formula C<sub>18</sub>H<sub>21</sub>BrN<sub>2</sub>O<sub>2</sub>·1/8 H<sub>2</sub>O, *M* = 379.53, colorless block 0.20 × 0.20 × 0.15 mm, *a* = 19.663(2) Å, *b* = 11.879(1) Å, *c* = 18.265(1) Å,  $\beta$  = 119.25(1)°, *V* = 3722.3(5) Å<sup>3</sup>,  $\rho_{\text{calcd}}$  = 1.354 g cm<sup>-3</sup>,  $\mu$  = 31.00 cm<sup>-1</sup>, empirical absorption correction via  $\psi$  scan data (0.576 ≤ *T* ≤ 0.654), *Z* = 8, monoclinic, space group *C2/c* (No. 15),  $\lambda$  = 1.54178 Å, *T* = 223 K,  $\omega/2\theta$  scans, 3932 reflections collected ( $\pm h$ , −*k*, −*l*), [(sin  $\theta$ )/ $\lambda$ ] = 0.62 Å<sup>-1</sup>, 3807 independent and 2261 observed reflections [*I* ≥ 2 $\sigma$ (*I*)], 222 refined parameters, *R* = 0.050, *wR*<sup>2</sup> = 0.149, maximum residual electron density 0.42 (−0.38) e Å<sup>-3</sup>. Hydrogens were found at the nitrogen atoms from difference Fourier calculations, others were calculated and refined as riding atoms. Data sets were collected with an Enraf Nonius CAD4 diffractometer. Programs used: Express, MolEN, SHELXs-97, SHELXL-97, SCHAKAL.

**Acknowledgment.** We thank the Deutsche Forschungsgemeinschaft, Heriot-Watt University, and Prof. Dr. G. Wulff for support, Ms. S. Johann for assistance in the preparation of starting materials, and Dr. R. Ferguson for the electrospray mass spectra.

**Supporting Information Available:** Detailed X-ray structural information on complex **3**, complex **3**·CDCl<sub>3</sub>, and complex **4**; concentration dependence of the amidine isomer ratio; time-, frequency- and temperature-dependent <sup>1</sup>H NMR and NOESY/EXSY spectra of **3** in CDCl<sub>3</sub>; additional line shape analysis results; ESI-MS of **3**. This material is available free of charge via the Internet at <http://pubs.acs.org>.

JO005632I

(32) Nishida, H.; Takada, N.; Yoshimura, M. *Bull. Chem. Soc. Jpn.* **1984**, *57*, 2600–2604.

(33) Grün, M. *Diplomarbeit*, University of Düsseldorf, 1996.

(34) Kraft, A.; Osterod, F.; Fröhlich, R. *J. Org. Chem.* **1999**, *64*, 6425–6433.

(35) Parker, R. A.; Kariya, T.; Grisar, J. M.; Petrow, V. *J. Med. Chem.* **1977**, *20*, 781–791.